applied sciences

MDPI

Article

Modular Bus Unit Scheduling for an Autonomous Transit System under Range and Charging Constraints

Hong Gao [1], Kai Liu [1,*], Jiangbo Wang [1] and Fangce Guo [2]

[1] School of Transportation and Logistics, Dalian University of Technology, Dalian 116024, China; gaohong9601@mail.dlut.edu.cn (H.G.); jiangbo_wang@dlut.edu.cn (J.W.)
[2] Urban Systems Lab (USL), Imperial College London, London SW7 2AZ, UK; fangce.guo@imperial.ac.uk
* Correspondence: liukai@dlut.edu.cn

Abstract: Recent advances in vehicle technology offer new opportunities for an electric, automated, modular bus (MB) unit with an adjustable capacity to be applied to transit systems, promising to tackle the resource allocation challenges of traditional buses in coping with uneven travel demand. Drawing on the concept of modular vehicles, this paper introduces a novel scheduling system in which MB units can be combined/separated from fulfilling imbalanced trip demands through capacity adjustments. We develop an optimization model for determining the optimal formation and trip sequence of MB units. In particular, given that the vehicles are electrically powered, battery range limits and charging plans are considered in the system scheduling process. A column-generation-based heuristic algorithm is designed to efficiently solve this model, with constraints related to travel demand and charging station capacity incorporated into the master problem and the trip sequence for modular units with limited energy solved by the subproblem. Taking real data from transit operations for numerical examples, the proposed model performs well in terms of both algorithmic performance and practical applications. The generated optimal MB dispatching scheme can significantly reduce the operating cost from $1534.31 to $1144.26, a decrease of approximately 25% compared to conventional electric buses. The sensitivity analysis on the MB dispatch cost and battery capacity provides some insights for both the scenario configuration and the battery selection for MB system implementation.

Keywords: modular bus; multi-trip scheduling; dynamic capacity adjustment; energy limitation; charging decision

Citation: Gao, H.; Liu, K.; Wang, J.; Guo, F. Modular Bus Unit Scheduling for an Autonomous Transit System under Range and Charging Constraints. *Appl. Sci.* **2023**, *13*, 7661. https://doi.org/10.3390/app13137661

Academic Editors: Jose Ramon Serrano, Alfredo Gimelli, Daniela Anna Misul and Gabriele Di Blasio

Received: 29 April 2023
Revised: 18 June 2023
Accepted: 26 June 2023
Published: 28 June 2023

1. Introduction

In light of the ongoing trend towards urbanization and population growth, the integration of electrified public transportation has emerged as a critical component in cities worldwide. Serving as a sustainable mode of transportation, it not only reduces traffic congestion and air pollution but also affords greater convenience for commuters [1]. However, establishing and sustaining a highly efficient and dependable electrified public transportation system is an intricate undertaking that involves multifarious factors such as network design, timetable preparation, vehicle scheduling, personnel allocation, and charging arrangements [2,3]. Among these factors, vehicle scheduling is an indispensable element that determines the quality of service and cost-effectiveness of the public transportation system [4]. Despite the widespread adoption of traditional fixed-route and fixed-capacity vehicle scheduling methods that allocate a predetermined number of vehicles to fixed routes, such approaches may be insufficiently adaptable to meet the dynamic requirements of travel demands, resulting in suboptimal resource allocation [5,6].

To optimize the provision of public transportation vehicles, it is imperative to account for the variability in demand across different trips and to leverage resource sharing and reallocation as necessary. MB units in Figure 1, also known as automated modular vehicles, constitute a novel vehicle technology that can dynamically adjust the capacity and size of platoons by assembling or separating different modules [7,8]. Particularly in transportation scheduling systems characterized by multiple trips, MB units can be customized to match passenger numbers and minimize the waste of vehicle resources and road congestion. For instance, modular units can be extracted from trips with lower demand and form large capacity MB platoons for trips with higher passenger demand, leading to cost-effective resource utilization [9,10]. In recent years, modular bus technology is now being validated in certain real-world applications, such as the United Arab Emirates [11] and Germany [12].

Figure 1. Modular bus unit (Source: http://www.next-future-mobility.com/ (accessed on 5 February 2023)).

Currently, modular bus-related research has been explored in multiple aspects, including optimization of schedule strategy optimization, passenger transfer plan design [13,14], specialized station deployment for modular unit reorganization [15], and driving trajectory planning [16]. Various studies collectively indicate that the concept of modular buses holds promise in reducing operating costs, improving service quality, and enabling more flexible vehicle dispatching, thereby potentially serving as an effective solution to address resource allocation challenges in traditional bus systems [17].

With respect to modular bus schedules relevant to the present research, the majority of studies have emphasized the optimization of MB platoon capacity and departure timetables in transit systems. Chen et al. [18,19], Dai et al. [20], Ji et al. [21], and Liu et al. [22] addressed when and how many modular buses to dispatch on a single bus route to minimize passenger waiting time and vehicle operating costs. Pei et al. [23] extended it to a network encompassing multiple bus stations, and Dakic et al. [24] optimized the composition and serve frequency of MB units and conventional buses on multiple lines. However, most of these studies primarily focus on the operation of a single-vehicle platoon composed of different numbers of modular units on the bus route or network, neglecting the more complex coupling/decoupling mechanisms among multiple MB platoons in a bus network scheduling system.

Furthermore, Shi et al. [25,26] and Zhang et al. [27] considered the interplay between MB platoons in the scheduling process. The former incorporated passenger arrival times to devise optimal departure times and node separation strategies for module vehicles in Y-shaped shared corridors, minimizing both passengers waiting time and vehicle dispatching costs. The latter has leveraged a modular transit network to expand service coverage, whereby only the coupling/decoupling of main modules, trailer modules, and passengers with impeccably aligned itineraries are deemed valid scheduling operations.

Evidently, in scenarios where multiple modular bus platoons coexist in the network, the coupling/decoupling operations can only be effectuated when the MB platoons or units converge at the same location and conform to time constraints, while the uneven demand between trips also emerges as a pivotal factor influencing the coupling/decoupling operations.

However, the aforementioned studies have largely overlooked the energy limitations and charging arrangement of electric-powered modular buses. It is well known that charging strategies, influenced by factors such as charging time, charging station capacity, and power resources, are crucial for the sustainable operation of electrified transportation systems [28–31]. In comparison to conventional buses, MB units are characterized by smaller sizes and battery capacities. Consequently, in the midst of demanding trip tasks, scheduling plans must not only account for fluctuations in passenger demand between trips but also ensure that the consumption energy of MBs during their travel sequence does not exceed the battery's capacity while flexibly devising charging plans to avert situations of insufficient power.

To bridge the gaps, we propose a modular bus scheduling system under range and charging constraints to reduce system costs while enhancing scheduling flexibility. Given that MB scheduling falls under the category of vehicle scheduling problems, wherein a group of modular buses needs to be efficiently assigned tasks under timetable constraints, we can draw insights from existing research on electric buses.

Two main categories of modeling methods can be identified. One is mainly based on a directed network to model the scheduling problem. Li [32] and Tang et al. [33] developed a spatiotemporal network graph and scheduling model for electric buses, in which charging stations are treated as time nodes. The arc-based model in their study can be solved by commercial solvers (GUROBI or CPLEX), while the path-based model is solved by a branch-and-price framework. Liu et al. [34] also models based on spatiotemporal graphs, except that a genetic algorithm solution method is adopted. In addition, there are some studies that extend the spatiotemporal graph to a complex network covering both vehicle and passenger flow [35]. Another category directly models the schedule regarding electric buses. Olsen et al. [36] proposed a mathematical model that simultaneously optimizes the charging station locations and scheduling schemes and solved it using a variable neighborhood search algorithm. Liu et al. [37] considered the impact of vehicle procurement costs, operating costs, and charging facility installation costs to establish a regional schedule model for electric buses. Rinaldi et al. [38,39] proposed mixed integer linear programming to address the mixed bus fleet scheduling problem, taking into account timetables and energy constraints.

The modeling method based on a directed network graph, as a focal point of our study, provides more precise sequential relationships among trips, vehicles, and charging processes. However, it is not entirely applicable to the MB scheduling problem, as a conventional bus can cover one trip with fixed capacity, whereas there is a coupling between MB platoons leading to dynamic capacity. In brief, we establish a modular bus unit scheduling model and method under range and charging constraints to achieve sustainability and economy of the transit system. Our contributions are as follows:

- The optimization model for determining the optimal formation and trip sequences of MB units is developed. In particular, given that the vehicles are electrically powered, battery range limits and charging plans are considered in the system scheduling process.
- A column generation-based heuristic algorithm is designed to efficiently solve this model. The constraints of trip demand and charging station capacity are included in the main problem, and the problem of the mileage of modular units under a limited range is solved by subproblems.
- Taking real data from transit operations for numerical examples, the proposed model performs well in terms of both algorithmic performance and practical applications, enabling strategic support for the promotion of modular bus technology in transit systems.

The rest of this paper is organized as follows: Section 2 presents the scheduling model for modular units in detail. Next, Section 3 elucidates a column generation-based heuristic algorithm. Section 4 introduces the case analysis and computational results in actual bus networks. The main conclusions are highlighted in Section 5.

2. Modular Bus Scheduling Model

2.1. Preliminaries

All notations involved in the model are listed in Abbreviations. The modular bus unit scheduling problem under range and charging constraints can be formally defined as follows. Given a directed graph $G = (N, A)$, the set of nodes $N = \{o\} \cup D \cup K \cup F \cup \{s\}$ is partitioned into the source node o (depot departure), the set D of dummy depot nodes providing temporary stay for buses, the set K of trips, the set F of time-expanded charging stations, and the sink node s (depot arrival). Each node $i \in N$ is equipped with the start time v_i, end time w_i, node demand d_i, node distance l_i and node energy consumption p_i. Without loss of generality, we assume that the demand, distance, and energy consumption of node $i \in N \backslash K$ are equal to zero, i.e., $d_i = 0, l_i = 0, p_i = 0, i \in N \backslash K$. The arc set A contains feasible arcs linking different nodes i and j, denoted as $(i, j) \in A$. Each arc (i,j) has an idle time t_{ij} and an arc energy consumption p_{ij}.

The connection rules of feasible arcs are shown in Table 1, distinguished between different nodes. The preprocessing of arcs can effectively reduce unnecessary connections and improve the model's efficiency. The feasibility condition of arc$(i, j) \in A, i, j \in D,\ i \neq j$ between virtual depot nodes is $w_i = v_j$ since all virtual depot nodes targeting the same depot do not have spatial location transfer, the dwell time for MB should be continuous. The arc leading from the origin o only makes sense for the case of going directly to the trip set K with the feasible condition $w_o + t_{oj} \leq v_j$. Similar connection rules exist for the arc to the endpoint s. For the feasibility condition $v_j - t_b \leq w_i + t_{ij} \leq v_j - t_a$, in addition to being governed by the end time w_i of the previous node i, the start time v_j of the subsequent node j and the idle time t_{ij}, it also comprises the waiting threshold t_b introduced to prevent the nodes from being visited prematurely, and the time t_a to ensure the smooth coupling/decoupling action between the MB units.

Table 1. The connection rules of feasible arcs.

<table>
<tr><th>j
i</th><th>o</th><th>D</th><th>K</th><th>F</th><th>s</th></tr>
<tr><td>o</td><td>×</td><td>×</td><td>$w_o + t_{oj} \leq v_j$</td><td>×</td><td>×</td></tr>
<tr><td>D</td><td>×</td><td>$w_i = v_j$</td><td colspan="2">$v_j - t_b \leq w_i + t_{ij} \leq v_j - t_a$</td><td>×</td></tr>
<tr><td>K</td><td>×</td><td colspan="3">$v_j - t_b \leq w_i + t_{ij} \leq v_j - t_a$</td><td rowspan="2">$w_i + t_{is} \leq v_s$</td></tr>
<tr><td>F</td><td>×</td><td colspan="2">$v_j - t_b \leq w_i + t_{ij} \leq v_j - t_a$</td><td>×</td></tr>
<tr><td>s</td><td>×</td><td>×</td><td>×</td><td>×</td><td>×</td></tr>
</table>

An example consisting of five node types o, D, K, F, s, and some feasible arcs, is used to illustrate the process of constructing the underlying network, as depicted in Figure 2. The travel time along each arc, the duration of nodes, and the sampling interval for charging nodes and virtual charging nodes are all set to one unit. A maximum waiting time of 2 units is allowed outside the depot, while the coupling and decoupling time for vehicles is set to 0.5 units. Starting from the source node o, two sets of trip sequences connected by feasible arcs are generated according to the connectivity rules. In the sequence $o - k_1 - k_3 - d_6 - d_7 - k_6 - s$, trips k_3 and k_6 are not directly connected because $11 - 2 \geq 5 + 1$, which would result in prolonged waiting times for MBs outside the depot. In contrast, modular buses can briefly pause at the virtual depot node after completing trip k_3 and then proceed to complete trip k_6. It is important to note that the virtual nodes d_6 and d_7 are both associated with the same depot, thus satisfying condition $8 = 8$.

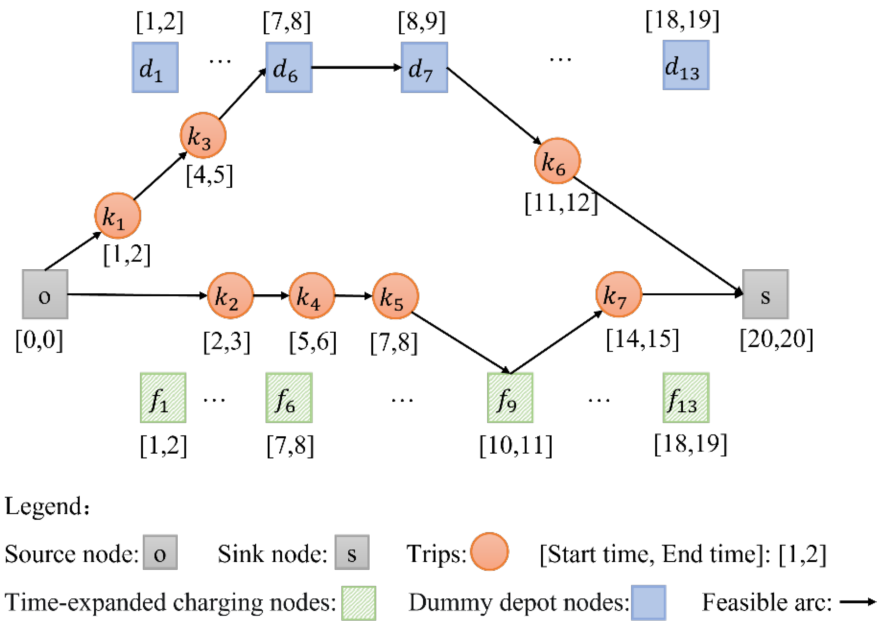

Figure 2. An example of the scheduling pictorial graph.

Another sequence $o - k_2 - k_4 - k_5 - f_9 - k_7 - s$ encompasses the process of trip execution and charging, where all the arcs involved satisfy the connectivity condition $v_j - t_b \leq w_i + t_{ij} \leq v_j - t_a$. For example, considering the arc (f_9, k_7), the modular unit arrives at node k_7 at time $11 + 1$, which is both earlier than the start time of node $k_7(14 - 0.5)$ and not earlier than $14 - 2$, as expressed by $14 - 2 \leq 11 + 1 \leq 14 - 0.5$.

The cost of a modular bus passing through arc c_{ij}, is also discussed by case depending on the node type, as defined below, where c_m represents the dispatch cost of one modular unit, c_p is the charging cost, and the remaining parameters c_t, c_s, and c_w are the idling cost, operating cost, and waiting cost per unit of time, respectively.

$$c_{ij} = \begin{cases} c_m + c_t \cdot t_{ij} + c_s \cdot (w_j - v_j), & (i,j) \in A, i = o \\ c_t \cdot t_{ij} + c_w \cdot (v_j - w_i - t_{ij}) + c_s \cdot (w_j - v_j), & (i,j) \in A, j \in K \\ c_t \cdot t_{ij} + c_w \cdot (v_j - w_i - t_{ij}), & (i,j) \in A, j \in D, \\ c_t \cdot t_{ij} + c_w \cdot (v_j - w_i - t_{ij}) + c_p, & (i,j) \in A, j \in F \\ c_t \cdot t_{ij}, & (i,j) \in A, j = d \end{cases}$$

2.2. Mathematical Formulation

We now formulate an arc-based model for the MB unit scheduling problem, which will be exploited in the Dantzig–Wolfe decomposition posited in the next section.

$$min \sum_{h \in H} \sum_{(i,j) \in A} c_{ij} \cdot x_{ijh} \cdot \delta_h \tag{1}$$

$$\sum_{j \in N^-(i)} x_{jih} = \sum_{j \in N^+(i)} x_{ijh} \leq 1 \qquad \forall i \in K \cup D \cup F, \forall h \in H \tag{2}$$

$$\sum_{j \in N^+(o)} x_{ojh} = \sum_{j \in N^-(s)} x_{jsh} \leq 1 \qquad \forall h \in H \tag{3}$$

$$q_{ih} = 0 \qquad \forall i \in \{o\} \cup F, \forall h \in H \tag{4}$$

$$q_{ih} = \sum_{j \in N^-(i)} \left(q_{jh} + p_{ji} \cdot \delta_h + p_i \cdot \delta_h \right) \cdot x_{jih} \qquad \forall i \in K \cup D, \forall h \in H \tag{5}$$

$$q_{ih} + \sum_{j \in N^+(i)} p_{ij} \cdot \delta_h \cdot x_{ijh} \le Q \cdot \delta_h \cdot \mu \quad \forall i \in N, \forall h \in H \tag{6}$$

$$\sum_{h \in H} \sum_{j \in N^-(i)} x_{jih} \cdot \delta_h \ge \lceil d_i / M \rceil \quad \forall i \in K \tag{7}$$

$$\sum_{h \in H} \sum_{j \in N^-(i)} x_{jih} \cdot \delta_h + \sum_{a=1}^{a_{max}} \sum_{h \in H} \sum_{j \in N^-(Y_i^a)} x_{j(Y_i^a)h} \cdot \delta_h \le U \quad \forall i \in F \tag{8}$$

$$x_{jih} \in \{0, 1\} \; \forall (i, j) \in A, \forall h \in H \tag{9}$$

The objective function (1) aims at minimizing the total system cost inclusive of various components such as dispatching costs, operation costs, and charging costs. Constraint (2) ensures that each MB platoon h remains balanced with respect to incoming and outgoing arcs at any given node $i \in K \cup D \cup F$. Constraint (3) specifies that once dispatched, an MB platoon h must depart from source o and return to node s. Constraints (4)–(6) define the energy limitations and charging plans for platoon h. Specifically, Constraint (4) states that the cumulative energy consumption at depot o and charging nodes should be zero, indicating that module platoon h can reset its energy through strategic charging decisions. Constraints (5) formulate q_{ih} at the nodes $i \in K \cup D$, determined jointly by the preorder node j and energy consumption on arc (j, i) and node i. The energy limitation of each module platoon should be met, and thus, Constraint (6) applies. A minimum number of MB units that serve trip i is imposed by constraints (7), where for coupling/decoupling action, the same location required is fulfilled by the node itself, and the time restrictions have been handled in the arc feasibility rules. Constraint (8) considers the charging station capacity, determined by the total number of module vehicles accessing node $i \in F$ and in the previous a_{max} charging nodes.

3. Solution Algorithm

Although GUROBI can be applied directly to the arc-based formulation, after some preliminary experiments, we find that the instance size handled by the solver is quite limited. To obtain the optimal solution for larger instances, we reformulate the MB scheduling problem as a path-based formulation. By applying Dantzig–Wolfe decomposition, the original problem effectively yields a master problem allocating MB platoons and a subproblem that addresses the trip sequences under range and charging constraints.

3.1. Master Problem

We define the following master problem:

$$min \sum_{r \in R} C_r \cdot Z_r \tag{10}$$

$$\sum_{r \in R} V_{ri} \cdot Z_r \ge \lceil d_i / M \rceil \quad \forall i \in K \tag{11}$$

$$\sum_{r \in R} V_{ri} \cdot Z_r + \sum_{r \in R} \sum_{a=1}^{a_{max}} V_{r(Y_i^a)} \cdot Z_r \le U \quad \forall i \in F \tag{12}$$

$$Z_r \in \{0,\ 1,\ 2,\ \ldots, g_{max}\} \tag{13}$$

where C_r means the cost of the trip sequence $r \in R$, V_{ri} is given as a parameter with $V_{ri} = 1$ if node i is covered by the trip sequence r provided by the pricing subproblem and 0 otherwise. Z_r, an integer variable, reveals the number of MB units assigned to the sequence r.

The master problem aims to minimize the total cost of the scheduling system by allocating varying numbers of MBs to the generated trip sequence, as indicated by constraint (10). Constraint (11) indicates that the total number of modular buses allocated to sequence r covering trip i is at least $\lceil d_i/M \rceil$. Constraint (12) guarantees that the number of modular units serviced at the charging station does not exceed its capacity. Constraint (13) imposes an integer constraint on variable $Z_r \in \{0,\ 1,\ 2,\ \ldots, g_{max}\}$.

3.2. Pricing Subproblems

Given a dual solution from the relaxed master problem, the pricing subproblem is set to find trip sequence r with a negative reduced cost. Solving the subproblem is essentially akin to enumerating all feasible trip sequences. Since all MB units are identical, the pricing subproblem associated with each bus can be expressed as:

$$min \sum_{(i,j)\in A} c_{ij}\cdot x_{ij} - \sum_{i\in K} V_{ri}\cdot\theta_i - \sum_{i\in F} V_{ri}\cdot\left[\omega_i + \sum_{a=1}^{a_{max}} w_{(Y_i^a)}\right] \tag{14}$$

$$\sum_{j\in N^-(i)} x_{ji} = \sum_{j\in N^+(i)} x_{ij} \le 1 \qquad \forall i \in K\cup D\cup F \tag{15}$$

$$\sum_{j\in N^+(o)} x_{oj} = \sum_{j\in N^-(s)} x_{js} = 1 \tag{16}$$

$$q_i = 0 \qquad \forall i \in \{o\}\cup F \tag{17}$$

$$q_i = \sum_{j\in N^-(i)} (q_j + p_{ji} + p_i)\cdot x_{ji} \qquad \forall i \in K\cup D \tag{18}$$

$$q_i + \sum_{j\in N^+(i)} p_{ij}\cdot x_{ij} \le Q\cdot\mu \qquad \forall i \in N \tag{19}$$

$$x_{ij} \in \{0,\ 1\} \qquad \forall (i,j) \in A \tag{20}$$

Let θ_i for $\forall i \in K$ and ω_i for $\forall i \in F$ be the values of the dual variables associated with constraints (11) and (12), respectively. Then, the minimum reduced cost of trip sequence r can be calculated by Equation (14). Constraint (15) requires that each node can visit node $i \in K\cup D\cup F$ at most once. Constraint (16) restricts the trip sequence to start at node o and end at node s. Constraints (17) and (18) give expressions for the cumulative energy consumption of the modular bus at different node types. Constraint (19) specifies the upper limit of the cumulative energy consumption. Constraint (20) defines a binary decision variable that equals 1 if the MB unit traverses arc (i,j) and 0 otherwise.

3.3. Solution Procedure

In this subsection, we design a column-generation-based heuristic (CGBH) algorithm for tackling the path-based MB unit scheduling model under range and charging constraints. A detailed flow chart is provided in Figure 3, which can be explained in the following five steps.

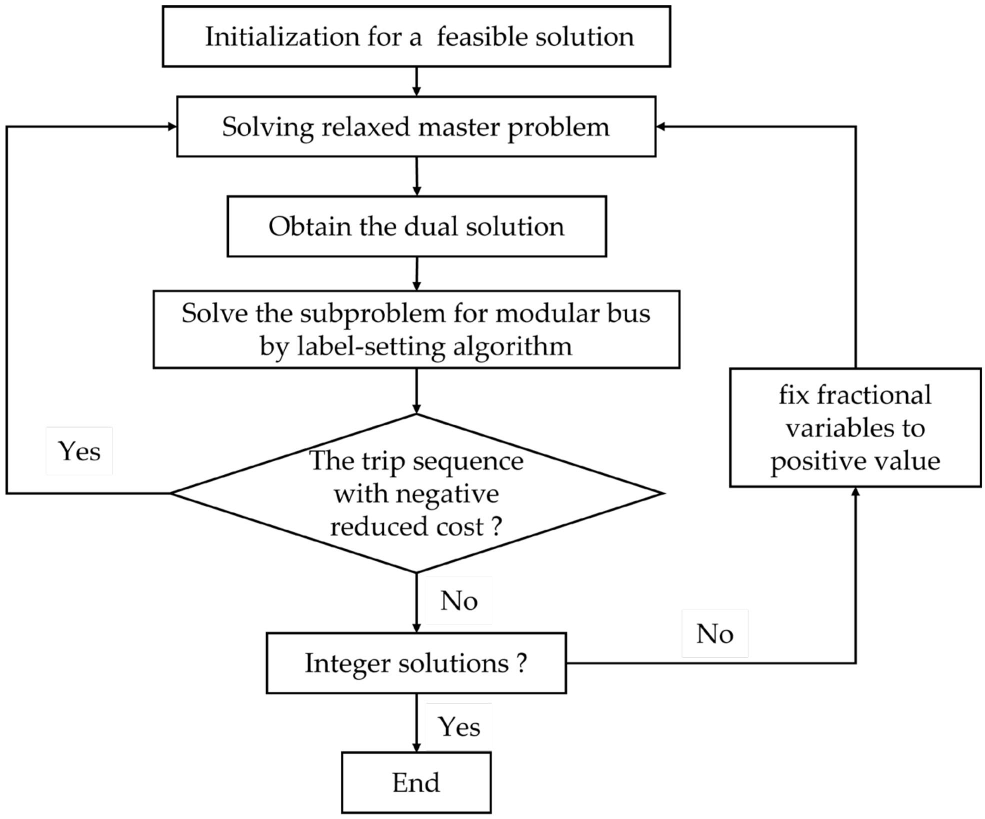

Figure 3. The flow chart of the column-generation-based heuristic algorithm.

Step 1: Initialization. Depending on the characteristics of the actual problem, a greedy algorithm can be employed to construct the columns that could potentially form a feasible solution.

Step 2: Obtain the dual solution. The initial solution is fed into the relaxed master problem to obtain the dual solutions of the constraints associated with trip nodes and charging nodes and then pass them to the subproblem.

Step 3: Solving the subproblem. The trip sequence with a negative reduced cost obtained from the subproblem is fed to the set R of the master problem. The label-setting algorithm is recognized as an effective approach for tackling these subproblems [40]. By leveraging the cost and energy consumption of nodes and arcs in the directed graph, the algorithm dynamically expands from node o to node s, generating labels that store cost and cumulative energy consumption information. Importantly, after each expansion, the algorithm performs a dominance test to compare the newly generated labels with existing labels in terms of cost and cumulative energy consumption. Labels that are dominated are deemed invalid and pruned, resulting in a streamlined label set and improved computational efficiency.

Step 4: Termination condition for iteration. The column generation process terminates when the newly generated trip sequence does not contribute to the objective function of the master problem, meaning there is no sequence r with a negative reduced cost.

Step 5: Obtaining integer solutions. The optimal solution obtained from the column generation process may be fractional. While the branch-and-price algorithm is commonly used to convert fractional solutions to optimal integer solutions [41], it can be time-consuming. In this study, a diving heuristic is adopted to obtain high-quality integer solutions. Based on the fractional solutions obtained, we selectively fix one or more fractional variables that are very close to integers to positive integer values and then invoke the column generation process until all solutions are integers.

4. Computational Results

In this section, we present the computational results obtained to validate the proposed model and algorithms. The real-world test scenarios and parameters in the experimental analysis are set in Section 4.1. Then, we report the performance of the CGBH algorithm in Section 4.2, followed by the scheduling scheme obtained in Section 4.3. In Section 4.4, we provide management insights regarding the impact of MB battery capacity and dispatch cost. All computational tests are performed on a computer with an Intel Core i7-8700 CPU processor, 8 GB RAM, and 3.2 GHz. The algorithm is coded in Python and relies on GUROBI 9.5.1 to solve the mathematical problem formulation.

4.1. Case Setup

Three in-service bus lines in Zhengzhou, China, with the same starting point and similar endpoints, were set as scheduling test scenarios, as shown in Figure 4. The close geographical locations among the lines make the application of scheduling schemes with multiple mixed trips more realistic and consistent with the research context of this study.

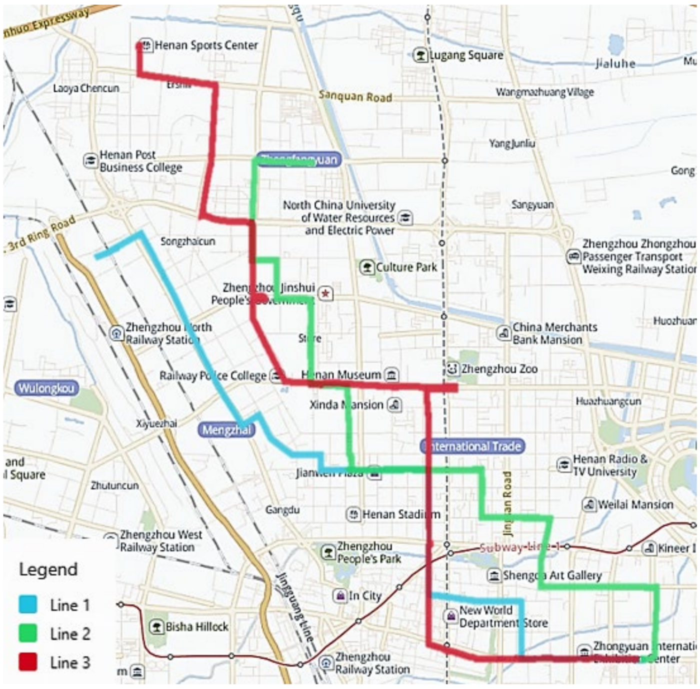

Figure 4. Test scenario of three in-service bus lines.

According to the research associated with the modular bus [20–23], we tune the parameters associated with the modular bus, including $c_m = \$10$ per vehicle, $c_t = \$3.43$ per hour, $c_s = \$5.72$ per hour, $c_p = \$3$, $c_w = \$1.72$ per hour, $Q = 30$ kWh, $\mu = 0.7$, $M = 15$ passengers, $U = 8$, $t_a = 3$ min, $t_b = 30$ min, $t_c = 10$ min.

The durations $w_i - v_i$ for different node types are set as follows: (1) $i = o$, $w_i - v_i = 0$; (2) $i \in K$, $w_i - v_i$ is determined by the actual operation time of the bus lines; (3) $i \in D$, $w_i - v_i = 30$ min; (4) $i \in F$, $w_i - v_i = 20$ min; (5) $i = s$, $w_i - v_i = \infty$.

Correspondingly, the current operating strategy of one electric bus (EB) covering one trip is used as the control group, and the relevant parameters are set as follows [28–31]. $c_m(\text{EB}) = \$97$ per vehicle, $c_t(\text{EB}) = \$12.34$ per hour, $c_s(\text{EB}) = \$20.56$ per hour, $c_p(\text{EB}) = \$25$, $c_w(\text{EB}) = \$6.17$ per hour, $Q(\text{EB}) = 250$ kWh, $\mu(\text{EB}) = 0.7$. Note that the meaning of the above parameters is the same as the definition in modular bus, with "(EB)" added to highlight the parameters associated with the electric bus.

4.2. Algorithm Efficiency

To test the effectiveness of the proposed algorithm, we extract four instances of progressively increasing size from the test scenario described in Section 4.1. Table 2 lists the results obtained by the commercial solver GUROBI and the CGBH algorithm on four instances. The node number is the total number of elements in the set N. Whether under the label "GUROBI" or "CGBH", we report the lower bound provided by the linear relaxation problem (column LB ($)), the best-known objective value obtained for a certain time (column Obj ($)), the solution time (column Time(s)) and the percentage gap (column Gap (%)), calculated by (Obj-LB)/Obj.

Table 2. Comparison results of the CGBH algorithm and GUROBI.

Instance			GUROBI				CGBH			
Number	**Trip**	**Node**	**LB ($)**	**Obj ($)**	**Time (s)**	**Gap (%)**	**LB ($)**	**Obj ($)**	**Time (s)**	**Gap (%)**
(1)	10	52	375.45	375.45	43.13	0.00	375.45	375.45	0.89	0.00
(2)	30	92	1106.22	1147.16	>7200	3.57	1144.26	1144.26	18.93	0.00
(3)	60	184	2166.27	2438.63	>7200	11.17	2213.68	2217.35	464.87	0.17
(4)	90	214	3094.25	4113.42	>7200	24.78	3207.08	3215.24	824.40	0.25

From Table 2, it is apparent that GUROBI is able to easily obtain optimal solutions that are identical to those obtained by the CGBH algorithm, but only in small-scale instances (1). However, as the size of the instances increases, GUROBI exhibits a significant discrepancy between the lower bound and best-known objective value, even consuming a longer time of more than 7200 s. In contrast, the column-generation-based heuristic algorithm consistently demonstrates favorable performance in terms of both solution time and gap, regardless of the instance size. Consequently, the algorithm proposed in this study shows remarkable efficiency and precision in solving the MB scheduling model.

4.3. Results and Analyses

Table 3 illustrates the optimal scheduling scheme for MB units in instance (2), where a total of 27 modular buses operates on 18 trip sequences to fulfill the demand of 30 trips. Note that in the "Trip Sequence" column, the numbers 1–30, 31–60, and 61–90 represent the 30 trip nodes, 30 temporary depot nodes, and 30 time-extended charging nodes, respectively. The symbols o and s are the source and sink, referring to the same depot.

Table 3. Optimal modular bus scheduling scheme.

Number	Trip Sequence	Number of Units Equipped with MB Platoon	Cumulative Energy Consumption (kWh)	Cost ($)
1	o-1-7-14-84-21-27-s	3	45.37	155.23
2	o-3-9-80-18-26-30-s	1	15.76	53.25
3	o-2-7-48-51-54-88-25-29-s	1	15.01	48.18
4	o-4-70-10-17-59-26-30-s	1	18.13	50.89
5	o-6-11-18-24-s	1	18.34	39.57
6	o-3-41-13-19-s	1	17.37	34.6
7	o-3-70-10-17-23-28-s	3	52.26	152.08
8	o-5-11-52-55-22-s	1	15.87	32.79
9	o-6-12-54-22-s	2	33.6	67.38
10	o-5-11-18-s	1	15.76	32.91
11	o-15-20-26-30-s	3	57.16	116.52
12	o-9-16-22-s	1	16.46	32.02
13	o-2-8-14-84-57-25-29-s	1	15.01	53.34
14	o-5-11-18-24-s	1	19.05	40.02
15	o-6-12-54-57-60-26-30-s	1	19.05	41.27

Table 3. *Cont.*

Number	Trip Sequence	Number of Units Equipped with MB Platoon	Cumulative Energy Consumption (kWh)	Cost ($)
16	*o*-2-8-77-17-23-28-*s*	1	15.16	50.17
17	*o*-1-68-9-16-22-*s*	1	16.46	43.25
18	*o*-4-41-13-19-*s*	3	52.13	100.79
Total	Satisfying the demands of 30 trips	27	Not exceeding the battery capacity	1144.26

First, compared to a traditional electric bus scheduling plan where one bus covers a single trip, the MB scheduling scheme reduces costs from $1534.31 to $1144.26, a decrease of approximately 25%, calculated by $(1534.31 - 1144.26)/1534.31 \times 100\% = 25\%$, effectively cutting operating expenses for the transit system.

Second, as elucidated in "Trip sequence", all trips can be categorized into two types. The first type encompasses trips that are covered by multiple sequences, exemplified by Trip 1 being served by both Sequence 1 and Sequence 17. This underscores the advantage of the coupling/decoupling mechanism of modular buses, wherein the consolidation of three MBs and one standalone MB results in four MB units effectively executing Trip 1, followed by their separation to serve subsequent trips. The other type of trip can be fully covered by a single MB platoon. For example, both Trip 21 with Demand 35 and Trip 27 with Demand 42 are only present in Trip Sequence 1, being covered directly by three modular buses with Capacity 45. Additionally, from the usage of charging nodes, the maximum number of MBs served in the occupied charging nodes 68, 70, 77, 80, 84, and 88 is 4, which does not exceed the maximum capacity of 8.

Finally, we further verify the effectiveness of the trip sequence. Taking Sequence 1 as an example, a modular platoon with three MB units departs from node o, executes trips 1, 7, and 14 in order, replenishes power at charging node 84, and subsequently executes Trips 21 and 27, finally returning to depot s. Notably, the cumulative energy consumption of this bus platoon amounts to 45.37 kWh, which falls below the effective battery capacity calculated as $30 \times 3 \times 0.7 = 63$ kWh, indicating the correctness of the energy consumption constraints and charging decisions. Analogously, other trip sequences are confirmed to be valid.

In terms of cost, the total cost of a trip sequence is generally determined by the nodes covered by the sequence and the number of assigned module bus platoons. If a trip sequence is assigned only one module unit, its cost is calculated by summing the arc costs that constitute the sequence. On the other hand, if the trip sequence is assigned multiple module buses, each cost item needs to be multiplied by the corresponding quantity to calculate the total cost of the sequence. It is evident that the cost can vary when different platoons are assigned to the same sequence. For example, in Table 3, the cost of the first sequence carrying three module buses is $155.23. However, if the same sequence is assigned one MB unit, the cost would be $155.23/3. Additionally, we have provided the costs of the trip sequences with the assigned platoons in the last column of Table 3, and the sum of these costs perfectly aligns with the objective function value obtained by our model, validating the accuracy of cost calculation.

4.4. Effects of the Dispatch Cost and Battery Capacity

This subsection is devoted to the sensitivity analyses of scheduling solution economics with respect to the dispatch cost and battery capacity.

Figure 5 illustrates the total costs of modular bus systems under various MB dispatch costs c_m. The solid lines in four different colors represent four instances, while the corresponding dashed lines denote the total costs of traditional buses only as a control group without fluctuations. From Figure 5, we observe that as the cost of MB units increases, the total cost of the dispatch system gradually rises at a relatively uniform rate. Taking modular bus instance (2) as an illustration, the difference between consecutive points, denoted as

C − A, represents the rate of change. When dispatching costs increase, the total number of modular buses dispatched and the scheme remain unchanged as modular buses are the sole vehicles involved in the scheduling process. Consequently, the increase in C − A, determined by the change value per modular bus ($5) multiplied by the total number of MB units in the instance, remains consistent throughout.

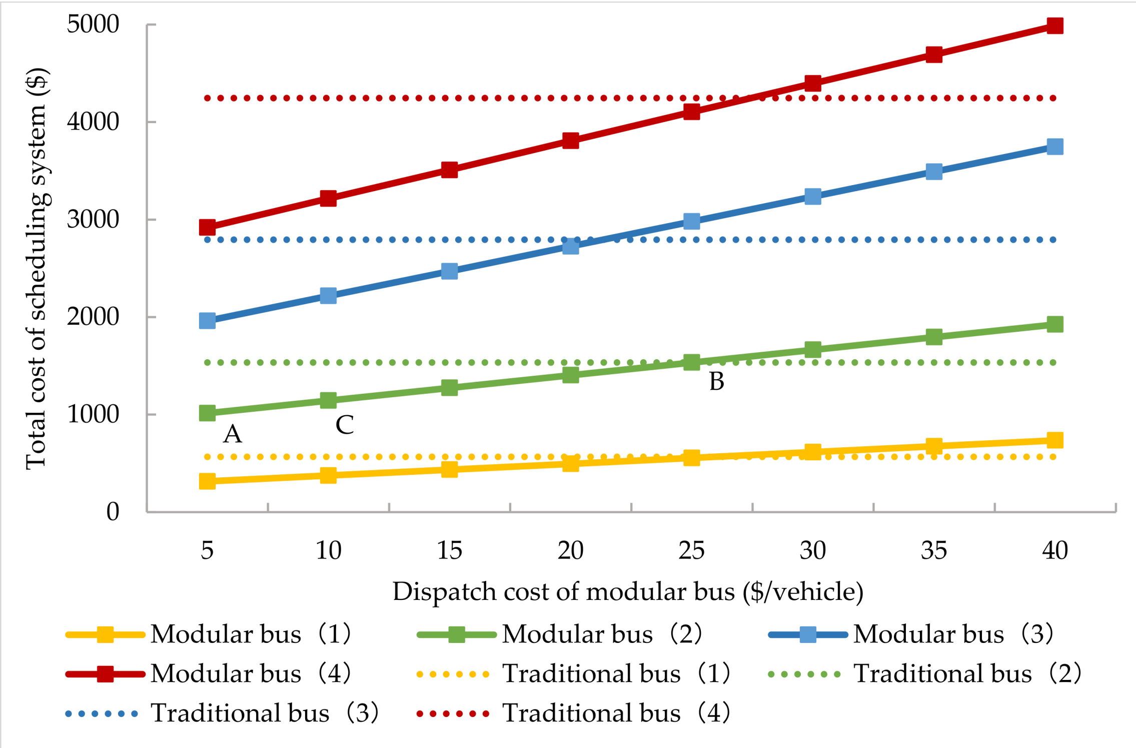

Figure 5. The impact of modular bus dispatching cost on total system cost.

Interestingly, the intersections between the solid line representing modular bus and the dashed line representing traditional bus vary across different instances. Specifically, in instances 1–4, these intersections occur at approximately $25, $25, $20, and $28 for the individual bus cost, respectively. This phenomenon primarily relates to the ratio of (B − A)/(C − A), as exemplified in instance 2. Here, B − A represents the overall cost gap between the traditional bus system and the modular bus system at a dispatching cost of $5, while C − A represents the cost difference between any two adjacent points.

The value of B − A signifies the economic gap between the two scheduling modes. When the modular bus scheduling mode better aligns with the trip organization and passenger demand in a given scenario compared to the fixed-capacity scheduling mode of traditional buses, a larger difference in B − A arises. We qualitatively speculate that in scenarios with low or fluctuating demand between trips, the fixed-capacity scheduling strategy of traditional buses is likely to result in wasted vehicle resources. In contrast, modular buses allow adjustments to capacity with coupling/decoupling techniques, thereby indicating an economic advantage. Based on the calculation of C − A (modular bus cost change step * total number of vehicles dispatched), the value of C − A is smaller when the fleet size is smaller.

In summary, it is crucial to identify the cost balance between the modular and traditional bus systems, which enables operators to make economically viable decisions by considering the cost range of the modular bus system. For instance, when the advantages of the modular bus system are pronounced, even in the early development stages with higher costs (reflected in a larger B − A value), it can still offer profitability compared to the traditional bus. As modular bus technology advances and the individual vehicle cost decreases substantially, the modular bus system will increasingly dominate as the preferred option.

Figure 6 depicts the impact of battery capacity, wherein the MB units system exhibits lower sensitivity to changes in battery capacity compared to Figure 5. This is because the impact of varying battery capacity on the bus dispatching strategy is indirect, resulting in only minor adjustments to the scheduling process. In contrast, changes in vehicle dispatch costs act directly on total vehicle dispatch costs, which represent a significant proportion of the system expenditure. It is worth noting that irrespective of the variations in battery capacity, even with a mere 15 kWh, the cost of the modular system remains lower than that of conventional bus systems. This underscores the prominent advantage of the modular bus scheduling mode.

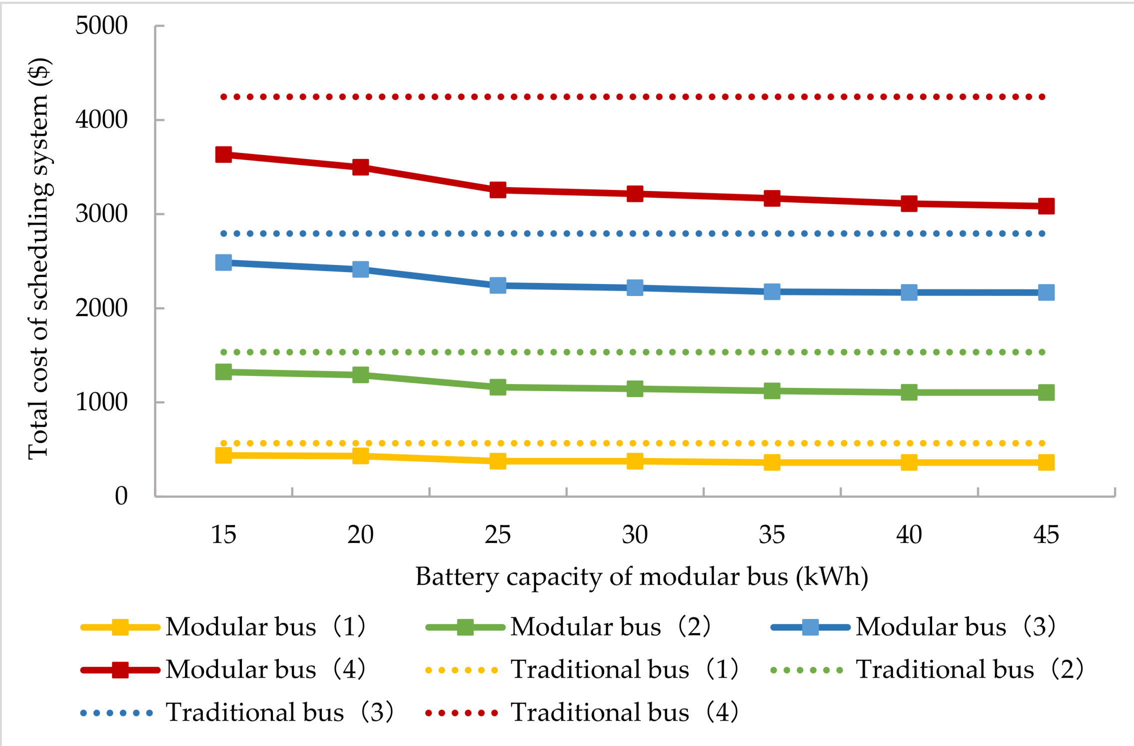

Figure 6. The impact of battery capacity on total system cost.

Furthermore, in Figure 6, the total system cost across the four instances gradually decreases and stabilizes as battery capacity increases. This trend can be attributed to the potential benefits of a longer battery range and reduced charging frequency. Specifically, a notable decrease in total cost is observed when battery capacity increases from 20 kWh to 25 kWh across all instances. This is explained by the larger battery capacity of modular buses covering more trips, thereby reducing the overall fleet size required and resulting in cost savings from fewer dispatched vehicles. For modular bus instance (2), increasing the battery capacity from 20 kWh to 25 kWh leads to a decrease in the number of vehicles from 36 to 28.

However, when the battery capacity surpasses 35 kWh, the cost fluctuation becomes insignificant, and blindly increasing battery capacity may actually result in higher battery costs. Therefore, we recommend procuring modular buses with a capacity between 25 kWh and 35 kWh, a range that allows the vehicle to operate efficiently without frequent recharging.

5. Concluding Remarks

A novel modular bus system is proposed to identify optimal formation, trip sequences, and charging decisions of modular vehicles, reducing operation costs while enhancing fleet scheduling flexibility. Through modeling and case validation, the key conclusions are as follows:

- The proposed column generation-based heuristic algorithm, which decomposes the original problem into a master problem and subproblems, outperforms widely used solvers in terms of time and computation speed. Even in a network of 214 nodes, the scheduling strategy can be obtained in about 10 min with a gap of less than 0.3%.
- The optimal modular bus scheduling scheme can reduce the overall system cost from $1534.31 to $1144.26, a reduction of approximately 25%, while accommodating uneven trip demand and embracing battery and charging station capacity constraints.
- Sensitivity analysis highlights the impact of dispatch cost and battery capacity of modular buses on system total costs. Compared to the traditional bus, operators are recommended to consider applying modular units in scenarios with low or volatile demand; there may still be scope for profitability even if the dispatching cost is high. Additionally, procuring modular buses with 25 kWh–35 kWh capacity can avoid frequent charging.

In future work, the reconfiguration of modular buses among stations beyond the ends of bus routes is a scalable research direction to improve fleet utilization and system economy. Additionally, fine consideration of the heterogeneous nature of energy consumption and charging processes among different modular units can further enhance system practicality. Incorporating the proposed column generation algorithm into a branch-and-price framework and finding diverse acceleration strategies for solving subproblems also merits in-depth exploration. Given the limitations of our research in practical applications, we will actively address real-world constraints and collaborate with ongoing electric and automated transportation projects to validate and improve our methodology.

Author Contributions: Conceptualization, methodology, software, visualization, investigation, writing—original draft, writing—review and editing. H.G. and K.L.; methodology, data curation, writing—review and editing, supervision, J.W.; conceptualization, writing—review and editing, F.G. All authors have read and agreed to the published version of the manuscript.

Funding: This research was funded by the National Natural Science Foundation of China (Grant Nos. 51378091 and 71871043).

Institutional Review Board Statement: Not applicable.

Informed Consent Statement: Not applicable.

Data Availability Statement: Not applicable.

Conflicts of Interest: The authors declare no conflict of interest.

Abbreviations

Notation list:
Sets

N:	The set of nodes, index by i or j
A:	The set of arcs, index by (i, j)
K:	The set of trips, index by i or j
D:	The set of dummy nodes providing temporary stay for modular vehicles, index by i or j
F:	The set of time-expanded charging stations, index by i or j
$N^+(i)$:	The set of nodes succeeding node i on the directed graph, G, that is $N^+(i) = \{j \in N \| (i, j) \in A\}$, index by i or j
$N^-(i)$:	The set of nodes preceding node i on the directed graph G, that is $N^-(i) = \{j \in N \| (j, i) \in A\}$, index by i or j
H:	The set of modular bus platoons, index by h
R:	The set of trip sequence, index by r

Parameters

o:	The source node (depot departure)
s:	The sink node (depot arrival)
v_i:	Start time of node i
w_i:	End time of node i
d_i:	Passenger demand of node i
l_i:	Distance of node i
p_i:	Energy consumption of node i
p_{ij}:	Energy consumption of arc $(i, j) \in A$
t_{ij}:	Idle time between node i and node j
t_a:	Constant threshold to ensure the smooth coupling/decoupling action between the modular bus units.
t_b:	Constant threshold introduced to prevent the nodes from being visited prematurely
c_{ij}:	Cost of a modular bus passing through arc (i, j)
c_m:	Dispatch cost of one modular unit
c_p:	Charging cost of the modular bus
c_t:	Idling cost per unit time of the modular bus
c_s:	Operating cost per unit time of the modular bus
c_w:	Waiting cost per unit time of the modular bus
δ_h:	The number of module units carried by module bus platoon h. $\delta_h \in \{1, 2, \ldots g_{max}\}$, where g_{max} is the maximum number of module units allowed to be carried
M:	Capacity of single modular bus
U:	Charging station capacity
Q:	Battery capacity of single modular bus
μ:	Battery loss rate
t_c:	Time interval between adjacent time-expanded charging nodes
Y_i^a:	The a-th node ahead of charging node i, where $a = 1, \ldots, a_{max}$, $a_{max} = \frac{w_i - v_i}{t_c}$
C_r:	Cost of the trip sequence r
V_{ri}:	$V_{ri} = 1$ if node i is covered by the trip sequence r provided by the subproblem and 0 otherwise
θ_i:	Values of the dual variables associated with constraints (11)
ω_i:	Values of the dual variables associated with constraints (12)

Variables

x_{ijh}:	Binary decision variable that equals 1 if module bus platoon $h \in H$ traverses arc (i, j), and 0 otherwise
q_{ih}:	Intermediate variables, denoting the cumulative energy consumption of the module bus platoon h at node i
Z_r:	Integer variable, reveals the number of modular bus units assigned to the sequence r
x_{ij}:	Binary decision variable that equals 1 if the modular bus traverses and 0 otherwise
q_i:	Intermediate variables, denoting the cumulative energy consumption of the module bus at node i

References

1. Badia, H.; Jenelius, E. Design and Operation of Feeder Systems in the Era of Automated and Electric Buses. *Transp. Res. Part A Policy Pract.* **2021**, *152*, 146–172. [CrossRef]
2. Perumal, S.S.G.; Lusby, R.M.; Larsen, J. Electric Bus Planning & Scheduling: A Review of Related Problems and Methodologies. *Eur. J. Oper. Res.* **2022**, *301*, 395–413. [CrossRef]
3. Häll, C.H.; Ceder, A.; Ekström, J.; Quttineh, N.-H. Adjustments of Public Transit Operations Planning Process for the Use of Electric Buses. *J. Intell. Transp. Syst.* **2019**, *23*, 216–230. [CrossRef]
4. Zhou, G.-J.; Xie, D.-F.; Zhao, X.-M.; Lu, C. Collaborative Optimization of Vehicle and Charging Scheduling for a Bus Fleet Mixed With Electric and Traditional Buses. *IEEE Access* **2020**, *8*, 8056–8072. [CrossRef]
5. Fu, L. Planning and Design of Flex-Route Transit Services. *Transp. Res. Rec.* **2002**, *1791*, 59–66. [CrossRef]
6. Quadrifoglio, L.; Dessouky, M.M.; Ordóñez, F. Mobility Allowance Shuttle Transit (MAST) Services: MIP Formulation and Strengthening with Logic Constraints. *Eur. J. Oper. Res.* **2008**, *185*, 481–494. [CrossRef]
7. NextFutureTransport. Available online: https://www.next-future-mobility.com/ (accessed on 5 February 2023).
8. Guo, Q.W.; Chow, J.Y.J.; Schonfeld, P. Stochastic Dynamic Switching in Fixed and Flexible Transit Services as Market Entry-Exit Real Options. *Transp. Res. Part C Emerg. Technol.* **2018**, *94*, 288–306. [CrossRef]

9. Gao, H.; Li, A.; Wang, J.; Liu, K.; Zhang, L. Design of an Intelligent Platoon Transit System towards Transportation Electrification. *World Electr. Veh. J.* **2022**, *13*, 153. [CrossRef]
10. Rau, A.; Tian, L.; Jain, M.; Xie, M.; Liu, T.; Zhou, Y. Dynamic Autonomous Road Transit (DART) for Use-Case Capacity More Than Bus. *Transp. Res. Procedia* **2019**, *41*, 812–823. [CrossRef]
11. Bold Business Editorial Team. Pods, The Self Driving Car Technology Can Be The Cure to Traffic Jams. 2017. Available online: https://www.boldbusiness.com/transportation/driverless-car-funding-grows/ (accessed on 28 April 2023).
12. Nehra, W. Berlin's Little Yellow Driverless Bus is Back! 2020. Available online: https://www.iamexpat.de/expat-info/german-expat-news/berlins-little-yellow-bus-back (accessed on 28 April 2023).
13. Caros, N.S.; Chow, J.Y.J. Day-to-Day Market Evaluation of Modular Autonomous Vehicle Fleet Operations with En-Route Transfers. *Transp. B* **2021**, *9*, 109–133. [CrossRef]
14. Wu, J.M.; Kulcsar, B.; Selpi; Qu, X.B. A Modular, Adaptive, and Autonomous Transit System (MAATS): An in-Motion Transfer Strategy and Performance Evaluation in Urban Grid Transit Networks. *Transp. Res. Part A Policy Pract.* **2021**, *151*, 81–98. [CrossRef]
15. Tian, Q.; Lin, Y.H.; Wang, D.Z.W.; Liu, Y. Planning for Modular-Vehicle Transit Service System: Model Formulation and Solution Methods. *Transp. Res. Part C Emerg. Technol.* **2022**, *138*, 103627. [CrossRef]
16. Li, Q.; Li, X. Trajectory Planning for Autonomous Modular Vehicle Docking and Autonomous Vehicle Platooning Operations. *Transp. Res. Part E Logist. Transp. Rev.* **2022**, *166*, 102886. [CrossRef]
17. Khan, Z.S.; He, W.; Menéndez, M. Application of Modular Vehicle Technology to Mitigate Bus Bunching. *Transp. Res. Part C Emerg. Technol.* **2023**, *146*, 103953. [CrossRef]
18. Chen, Z.; Li, X.; Zhou, X. Operational Design for Shuttle Systems with Modular Vehicles under Oversaturated Traffic: Discrete Modeling Method. *Transp. Res. Part B Methodol.* **2019**, *122*, 1–19. [CrossRef]
19. Chen, Z.; Li, X.; Zhou, X. Operational Design for Shuttle Systems with Modular Vehicles under Oversaturated Traffic: Continuous Modeling Method. *Transp. Res. Part B Methodol.* **2020**, *132*, 76–100. [CrossRef]
20. Dai, Z.; Liu, X.C.; Chen, X.; Ma, X. Joint Optimization of Scheduling and Capacity for Mixed Traffic with Autonomous and Human-Driven Buses: A Dynamic Programming Approach. *Transp. Res. Part C Emerg. Technol.* **2020**, *114*, 598–619. [CrossRef]
21. Ji, Y.; Liu, B.; Shen, Y.; Du, Y. Scheduling Strategy for Transit Routes with Modular Autonomous Vehicles. *Int. J. Transp. Sci. Technol.* **2021**, *10*, 121–135. [CrossRef]
22. Liu, X.; Qu, X.; Ma, X. Improving Flex-Route Transit Services with Modular Autonomous Vehicles. *Transp. Res. Part E Logist. Transp. Rev.* **2021**, *149*, 102331. [CrossRef]
23. Pei, M.; Lin, P.; Du, J.; Li, X.; Chen, Z. Vehicle Dispatching in Modular Transit Networks: A Mixed-Integer Nonlinear Programming Model. *Transp. Res. Part E Logist. Transp. Rev.* **2021**, *147*, 102240. [CrossRef]
24. Dakic, I.; Yang, K.; Menendez, M.; Chow, J.Y.J. On the Design of an Optimal Flexible Bus Dispatching System with Modular Bus Units: Using the Three-Dimensional Macroscopic Fundamental Diagram. *Transp. Res. Part B Methodol.* **2021**, *148*, 38–59. [CrossRef]
25. Shi, X.; Chen, Z.; Pei, M.; Li, X. Variable-Capacity Operations with Modular Transits for Shared-Use Corridors. *Transp. Res. Rec.* **2020**, *2674*, 230–244. [CrossRef]
26. Shi, X.; Li, X. Operations Design of Modular Vehicles on an Oversaturated Corridor with First-in, First-out Passenger Queueing. *Transp. Sci.* **2021**, *55*, 1187–1205. [CrossRef]
27. Zhang, Z.; Tafreshian, A.; Masoud, N. Modular Transit: Using Autonomy and Modularity to Improve Performance in Public Transportation. *Transp. Res. Part E Logist. Transp. Rev.* **2020**, *141*, 102033. [CrossRef]
28. Liu, K.; Gao, H.; Liang, Z.; Zhao, M.; Li, C. Optimal Charging Strategy for Large-Scale Electric Buses Considering Resource Constraints. *Transp. Res. Part D Transp. Environ.* **2021**, *99*, 103009. [CrossRef]
29. Liu, K.; Gao, H.; Wang, Y.; Feng, T.; Li, C. Robust Charging Strategies for Electric Bus Fleets under Energy Consumption Uncertainty. *Transp. Res. Part D Transp. Environ.* **2022**, *104*, 103215. [CrossRef]
30. Dougier, N.; Celik, B.; Chabi-Sika, S.-K.; Sechilariu, M.; Locment, F.; Emery, J. Modelling of Electric Bus Operation and Charging Process: Potential Contribution of Local Photovoltaic Production. *Appl. Sci.* **2023**, *13*, 4372. [CrossRef]
31. Zoltowska, I.; Lin, J. Optimal Charging Schedule Planning for Electric Buses Using Aggregated Day-Ahead Auction Bids. *Energies* **2021**, *14*, 4727. [CrossRef]
32. Li, J.Q. Transit Bus Scheduling with Limited Energy. *Transp. Sci.* **2014**, *48*, 521–539. [CrossRef]
33. Tang, X.; Lin, X.; He, F. Robust Scheduling Strategies of Electric Buses under Stochastic Traffic Conditions. *Transp. Res. Part C Emerg. Technol.* **2019**, *105*, 163–182. [CrossRef]
34. Liu, Y.; Yao, E.; Liu, S. Energy Consumption Optimization Model of Multi-Type Bus Operating Organization Based on Time-Space Network. *Appl. Sci.* **2019**, *9*, 3352. [CrossRef]
35. Li, L.; Lo, H.K.; Xiao, F. Mixed Bus Fleet Scheduling under Range and Refueling Constraints. *Transp. Res. Part C Emerg. Technol.* **2019**, *104*, 443–462. [CrossRef]
36. Olsen, N.; Kliewer, N. Location Planning of Charging Stations for Electric Buses in Public Transport Considering Vehicle Scheduling: A Variable Neighborhood Search Based Approach. *Appl. Sci.* **2022**, *12*, 3855. [CrossRef]
37. Liu, Y.; Yao, E.; Lu, M.; Yuan, L. Regional Electric Bus Driving Plan Optimization Algorithm Considering Charging Time Window. *Math. Probl. Eng.* **2019**, *2019*, 7863290. [CrossRef]

38. Rinaldi, M.; Picarelli, E.; D'Ariano, A.; Viti, F. Mixed-Fleet Single-Terminal Bus Scheduling Problem: Modelling, Solution Scheme and Potential Applications. *Omega* **2020**, *96*, 102070. [CrossRef]
39. Rinaldi, M.; Parisi, F.; Laskaris, G.; D'Ariano, A.; Viti, F. Optimal Dispatching of Electric and Hybrid Buses Subject to Scheduling and Charging Constraints. In Proceedings of the 2018 21st International Conference on Intelligent Transportation Systems (ITSC), Maui, HI, USA, 4–7 November 2018; pp. 41–46.
40. Irnich, S.; Desaulniers, G. *Shortest Path Problems with Resource Constraints BT—Column Generation*; Desaulniers, G., Desrosiers, J., Solomon, M.M., Eds.; Springer: Boston, MA, USA, 2005; pp. 33–65. ISBN 978-0-387-25486-9.
41. Barnhart, C.; Johnson, E.L.; Nemhauser, G.L.; Savelsbergh, M.W.P.; Vance, P.H. Branch-and-Price: Column Generation for Solving Huge Integer Programs. *Oper. Res.* **1998**, *46*, 316–329. [CrossRef]